J. Membrane Biol. 146, 59–71 (1995)

The Journal of
Membrane
Biology

Kinetic Analysis of Two Simultaneously Activated K^+ Currents in Root Cell Protoplasts of *Plantago media L.*

S.A. Vogelzang, H.B.A. Prins

ECOTRANS, Lab. of Plant Physiology, Dept. of Plant Biology, Biological Center, University of Groningen, P.O. box 14, 9750AA Haren, The Netherlands

Received: 19 October 1994/Revised: 28 February 1995

Abstract. Two different, simultaneously activated outward rectifying K^+ currents were analyzed in the plasmalemma of root cortex protoplasts of *Plantago media.* Their gating is dependent on the diffusion potential for K^+ (E_K). The threshold potential was more negative than E_K allowing small inward currents at potentials below E_K thereby keeping cells with little pump activity in the K state (Vogelzang & Prins, 1994).

Time and voltage dependence of the outward rectifying K^+ currents have been analyzed with Hodgkin-Huxley-like (HH) models. Dynamic responses of whole cell currents to pulse potentials were analyzed with two voltage dependent functions, the Boltzmann distribution for open probability per gate and the transition rate towards the open state (α). The transition rate in the opposite direction (β), was calculated from α and the Boltzmann distribution. These functions were used for an integral analysis of activation and deactivation currents measured over a range of pulse potentials. Both whole cell and single channel data were used for the determination of the number of closed and open states. The effects of single channel flickering on time response and amplitude of tail currents were added to the model. The dominant K^+ channel present in the plasmalemma of *P. media* has a characteristic nonlinear single channel *I-V* curve reducing the amplitude of whole cell currents at positive potentials. To compensate for this nonlinearity, a four state translocator model was added to the whole cell open probability model. The analysis presented here provides a general basis for the study and comparison of K^+ channel kinetics in plant protoplasts.

Key words: *Plantago media* — Whole cell — Root cells — Channel kinetics — Patch clamp — Hodgkin-Huxley

Correspondence to: H.B.A. Prins

Introduction

The membrane potential of *Plantago media* root cortex cells strongly depends on the K^+ concentration of the extracellular solution: in cells of excised roots (Maathuis & Prins, 1990) as well as in isolated root cortex protoplasts (Vogelzang & Prins, 1994). This is true for protoplasts and root cells in the potassium diffusion state (K state) and for isolated protoplasts in the pump state (P state). By definition cells in the K state have a membrane potential (V_m) equal to the Nernst potential for potassium (E_K) and cells in the P state have a V_m that is more negative than E_K (Bisson & Walker, 1982; Beilby, 1986; Cruz-Mireles & Ortega-Blake, 1991). For protoplasts in the P state V_m was about 90 mV more negative than E_K, within the range of 1 to 100 mM extracellular K^+ (Maathuis & Prins, 1990; Vogelzang & Prins, 1994).

The K state indicates the presence of a dominant K^+ conductance in the plasmalemma, as was confirmed in a detailed study of single channels in the cell-attached-patch (CAP) and out-side-out-patch (OOP) configuration (Vogelzang & Prins, 1994). The dominant depolarization activated ion channel appeared to be highly selective for potassium. Unlike most ion channels that conduct outward rectifying currents (ORC) it conducted both inward and outward currents in steady state and its gating was E_K-dependent. The ion channel was called outward rectifying flickering channel (ORC-f) because of the typical flickering of its inward current. The threshold of its voltage dependent activation (V_{thr}), shifted with E_K and was always more negative. Thereby the ORC-f also conducts small inward currents. The combination of outward and inward K^+ currents around E_K tends to clamp V_m at E_K in protoplasts and intact cells with little H^+-ATPase pump activity. A second outward rectifier was detected in OOP. It was named sub-picoSiemens outward rectifying channel or ORC-sp, because unitary

changes in current could not be detected (Vogelzang & Prins, 1994). The single channel data predicted a significant contribution of the ORC-sp to outward currents in the whole cell configuration. Starting point for the present analysis is the hypothesis that these two separate K^+ conducting ORCs dominate also in the whole cell configuration. A minimal model for the analysis of whole cell data of *P. media* root cortex cells therefore must contain these two channels. The outcome of this analysis clearly supports this starting hypothesis. Up to now K^+ sensing gating mechanisms in ion channels, conducting outward rectifying currents, have rarely been reported in plant cells (Skerret & Tyerman, 1994). Inward rectifying K^+ currents in starfish eggs described by Hagiwara, Miyazaki & Rosenthal (1976) have a gating mechanism that interacts with K^+ ions. Inward rectifying currents with a K^+-sensing gating mechanism were reported in guard cells of stomata by Schroeder and Fang (1991) and in barley aleurone protoplasts (Bush et al., 1988).

Schroeder (1989) and Van Duijn (1993) analyzed the kinetics of K^+ selective outward rectifying currents of respectively *Vicia faba* guard cells and tobacco suspension cells. Superficially their activation and deactivation curves looked very similar. However Van Duijn reported that the parameters describing the voltage dependent kinetics of outward rectifying currents of tobacco cells were very different from those of *V. faba* guard cells if fitted with the same model (Van Duijn, 1993).

In this study, we report on a kinetic analysis of the two parallel outward rectifying currents in the plasmalemma of *P. media* root cortex protoplasts. The kinetic model of the ORC-f includes five closed and one open state and the HH-model of the ORC-sp one closed and one open state. The set of current data used for the activation and deactivation analysis contained a wide range of pulse potentials to insure an integral analysis of the data (ensemble analysis). Flickering can significantly increase the time response of deactivation currents (Colquhoun & Hawkes, 1977) therefore flicker kinetics were analyzed and incorporated in the kinetic model for ORC-f. The model was further extended with a four-state translocator model that predicts the K^+ dependent current-voltage relationship of an open ORC-f (Vogelzang & Prins, 1994).

Cation channels with flicker kinetics during deactivation seem present in the plasma membrane of various plant cells. Root cells of *P. maritima* displayed channels with flicker kinetics and conductance identical with the ORC-f in *P. media* (Vogelzang & Prins, *unpublished results*). Schachtman, Tyermann & Terry (1991) reported the presence of flicker channels with an E_K dependent gating in wheat root cells. Terry, Tyermann & Findlay (1991) observed flicker channels in the plasmalemma of protoplasts derived from Amaranthus seedlings. Recently Blom and coworkers (Blom-Zandstra et al., 1994) observed flicker channels in tobacco (leaf) and sweet pepper (leaf and root). Preliminary data show that these cation channels do not share the same kinetics.

The present analysis provides a general biophysical basis for the study of K^+ channels responsible for the stable K-state of root cells. The maintenance of this K state in root cells may have a function as part of the K^+ transport system in plants. The depolarization activated K^+ conductances in the plasma membrane of *P. media* root cortex cells permit both net influx and net efflux of K^+. An outward proton current, generated by proton pump activity, can hyperpolarize V_m to potentials more negative than E_K causing an inward K^+ current. Complete deactivation of the K^+ conductance will only occur if the outward proton current is greater than the maximum steady state inward K^+ current. Outward K^+ currents occur if V_m is depolarized to potentials more positive than E_K, e.g., by the activation of anion conductances.

Materials and Methods

Isolation of Protoplasts

Root-cortex protoplasts of *Plantago media L.* were isolated using the method of Vogelzang and Prins (1992) yielding a rapid isolation of protoplasts after minimal exposure of the root tissue to cell wall degrading enzymes. The cortex cells were collected at the bottom of a specially prepared culture dish (Ince et al., 1985). Before the start of an experiment, the measuring chamber was perfused with the bath solution for 15 to 30 min removing all debris, while the protoplasts remained attached to the bottom of the dish.

Solutions

Unless noted otherwise, the solutions had the following composition. Bath medium (in mM): 350 Mannitol, 10 KCl, 2 $MgCl_2$, 2 $CaCl_2$, 5 MES, adjusted to pH 6.0 with 0.5 M BTP. Pipette medium (in mM): 230 Mannitol, 100 KCl, 2 $MgCl_2$, 0.1 $CaCl_2$, 1 K_4BAPTA (Sigma), 5 HEPES, adjusted to pH 7.2 with 0.5 M BTP. When potassium concentrations other than those mentioned above were used, osmolarity was kept constant with mannitol to 387 and 446 mOsm for bath and pipette solution, respectively.

Patch Clamp Experiments

Conventional patch clamp techniques were applied (Hamill et al., 1981) in the whole-cell and out-side-out-patch configuration with an EPC-7 patch clamp amplifier (List Electronics, Darmstadt, F.R.G.). Whole cell configurations were acquired by suction within 1 to 5 minutes after the obtainment of a gigaseal. The whole cell resistance was identified by the increase of capacity (0.72 $\mu F/cm^2$).

The reversal potential of whole cell *I-V* curves was determined after subtraction of the leak resistance. The leak resistance was assumed to be ohmic and was determined by linear fitting of the instantaneous currents for a range of pulse potentials starting from a holding potential where ion channel activity was minimal. The data were subsequently corrected for the current through this leak. The leak resistance typically was higher than 1GΩ. The ratio membrane conduc-

tance at E_K/leak conductance was always higher than 500, therefore leak subtraction was not critical for the determination of the reversal potential, V_r. Voltage and current data were transferred via a CED 1401 A/D-converter controlled by patch clamp software of CED (Cambridge, UK). Data were sampled at 1 to 12 kHz and stored on a personal computer (Olivetti M-24).

Calculations

For analysis of whole-cell channel recordings, (Turbo-Pascal) CED-compatible software (ECOpatch) was developed. The parameters of the Boltzmann distribution and α function were determined by coupling the simplex algorithm (Caceci, 1984) to Turbo Pascal matrix-handling graphical routines, written for this procedure. The standard error of the ensemble fit was calculated from the sum of residuals (Σd_i^2) by: $\sigma_{fit} = \sqrt{[\Sigma d_i^2/n(n-1)]}$. Calculated values are expressed as means ± SD.

Results

Depolarization Activated Inward-Outward Currents in Whole Cell

Figure 1 shows typical whole cell recordings of depolarization activated currents. An increase of the pulse potential from a holding potential of −100 mV to potentials ranging from −50 to +40 mV activated inward currents at potentials more negative than E_K (30 to 50 mV) and outward currents above E_K. The outward current was large compared with the inward current. The activation curve initially had a sigmoidal shape, thereafter activation was slower and a second single exponential increase could be identified. Apparently channels with different activation kinetics were activated.

Single Channel Origin of Whole Cell Currents

Figure 2 shows activation curves of outward rectifying currents through ion channels in OOP recordings and an ensemble average of 30 of these recordings. Examples hereof are displayed in the five upper traces. Earlier single-patch experiments (Vogelzang & Prins, 1994) led to our hypothesis that two K^+ conductances dominate, the fast ORC-f and the slow ORC-sp, and carry the outward current. In agreement with this hypothesis, the ensemble average shows a fast and a slow activation component corresponding to time responses in whole cell (Fig. 1). Activation of ORC-f at potentials 50 mV more positive than E_K is completed within a few seconds while activation of ORC-sp is five to ten times slower. Unitary current steps could not be detected for ORC-sp. Apparently the conductance of an individual ORC-sp channel is below the detection level of a conventional patch clamp amplifier (Vogelzang & Prins, 1994).

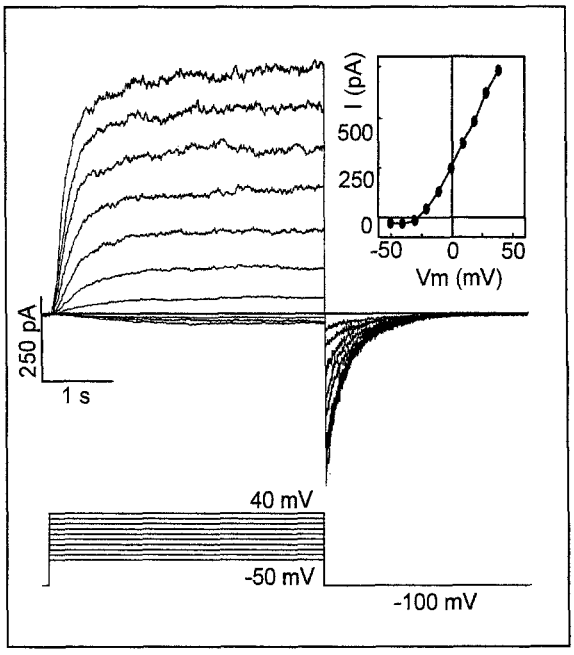

Fig. 1. Whole cell recordings of a *P. media* root protoplast. Outward rectifying currents were activated upon depolarizing pipette potentials. Pulses were applied ranging from −50 to 40 mV with 10 mV steps. Deactivation tail currents appeared when the voltage was returned to the holding potential of −100 mV. A leak subtraction of 12.5 GΩ has been applied to all tracks. The inset displays the corresponding whole cell current voltage curve measured at the end of each applied pulse (4 sec). Both small inward (−20 pA) and large outward (+750 pA) currents were conducted by the depolarization activated channels. The K^+ concentration of bath and pipette solution was 30 and 108 mM respectively.

E_K-Dependent Gating of Whole Cell Currents and K^+ Selectivity

Whole cell recordings of depolarization activated currents were made at different E_K values. In Figure 3*A*, two examples of the resulting *I-V* curves are depicted. Both curves show, besides the large outward going current, a small but significant inward current at potentials more negative than their reversal potential (V_r). In Figure 3*B*, the reversal potentials of whole cell *I-V* curves from twelve different protoplasts have been plotted versus E_K (Correl.Coeff. = 0.99). The V_r of the *I-V* curves almost equalled E_K (Fig. 3*B*). The ratio membrane conductance at E_K/leak conductance was always higher than 500, therefore the leak had no significant effect on V_r. Figure 3*A* also shows that V_{thr} is close to E_K-50 mV and that V_{thr} shifts along the abscissa with E_K. Apparently both conductances, ORC-f and ORC-sp, have a K^+-sensing gating mechanism. This is in agreement with the results from single channel analysis of OOP recordings (Vogelzang & Prins, 1994).

Figure 4 shows the effect of the K^+ channel blocker TEA. Addition of 50 µL 2M TEA, final concentration 100 mM, resulted in a complete block within 10 min (Fig.

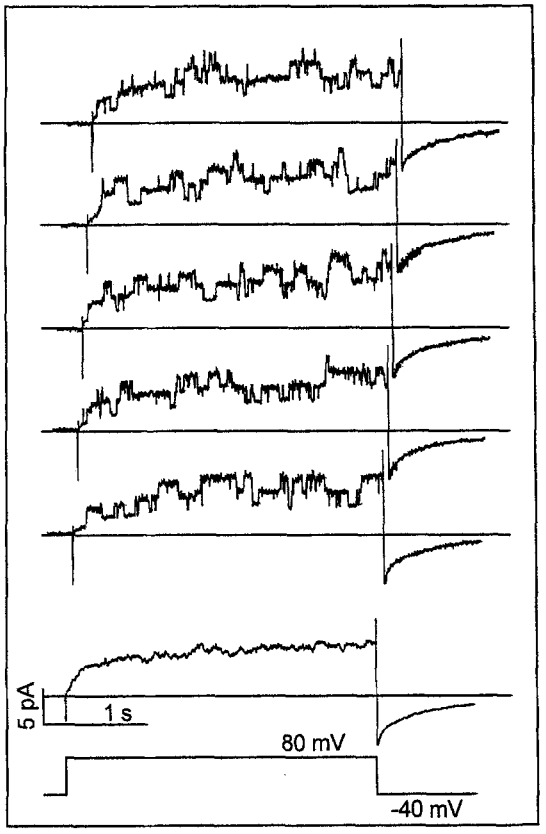

Fig. 2. Single channel events in the outside out patch configuration showing the activation of at least four outward rectifying ion channels. The Holding potential was –40 mV, the applied pulse step 80 mV. Note the slow increase of the baseline that raises the level of the ion channel currents in a single exponential manner. The five upper traces are randomly selected from a group of thirty records. The lower trace is the result of an ensemble average of these thirty records. It displays a biphasic activation of the current followed by a single exponential deactivation curve.

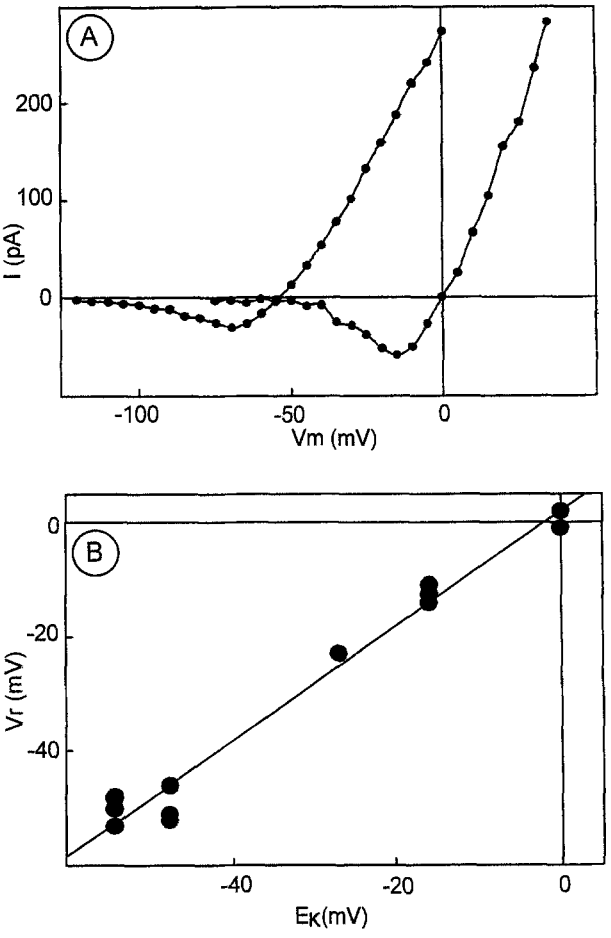

Fig. 3. (*A*) Whole cell *I-V* curves of two *P. media* root protoplast with different Nernst potentials for potassium (E_K). The left- and right-handed curve are from protoplasts with an E_K of –55 and 0 mV respectively. Leak was subtracted from both curves (5 & 2 GΩ respectively). (*B*) The reversal potential (V_r) of twelve whole cell *I-V* curves from different cells are plotted versus their calculated E_K value.

4*B*). Earlier OOP experiments showed that a complete block of the K^+ channels could be obtained with 50 mM TEA (Vogelzang & Prins, 1994). In these experiments the controle solution was exchanged for a TEA containing one. In the whole cell configuration, however, we could not use this method without loosing the seal. Therefore TEA was added to the solution. To obtain nevertheless a complete block within a reasonable time period we needed a much higher TEA concentration as it diffused only slowly to the protoplast. Even with 100 mM TEA it took 10 min to reach complete inhibition (Fig. 4*C*). The effect of TEA indicates that both the ORC-f and the ORC-sp are selective for potassium, as was already indicated by V_r being equal to E_K. Figure 4*C* shows the effect of TEA in time. *I-V* curves with identical pulse protocols were made before and after addition of TEA. The currents through both conductances were reduced at the same rate. Addition of TEA resulted in a single exponential decrease of the nominal outward currents while the shape of *I-V* curves remained essentially the same.

Open Probability and Transition Rates: Voltage Dependence of Ion Channel Gating

Ion channels have the capability of undergoing rapid conformational changes between conducting (open) and nonconducting (closed) states. For many ion channels the transition rates are voltage dependent. α and β represent rate constants for the transition from respectively closed to open and open to closed:

$$C \underset{\beta}{\overset{\alpha}{\rightleftarrows}} O \qquad \text{Scheme 1}$$

The conformational changes are generally assumed to be

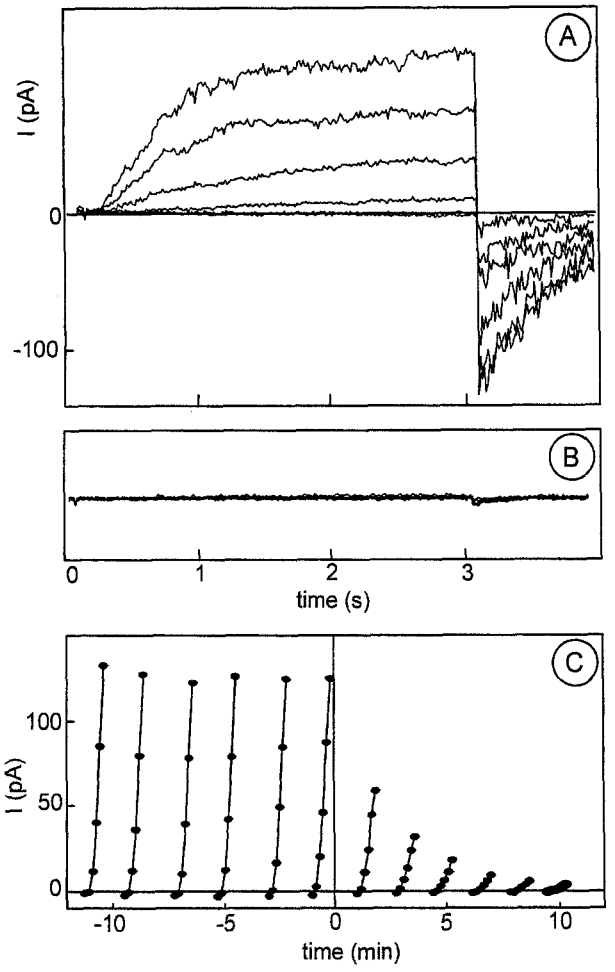

Fig. 4. (*A*) Whole cell recordings of a *P. media* root protoplast before the addition of TEA to the bath solution. Outward rectifying currents were activated upon depolarizing pipette potentials. Pulses were applied ranging from –90 mV to 30 mV with 20 mV steps. The holding potential was –170 mV. (*B*) The response of the same protoplast ten min after the addition of 50 µl TEA (2 M) to the bath solution, resulting in a final concentration of 100 mM TEA. (*C*) Successive *I-V* curves showing a stable noninactivating response to depolarizing pulse potentials before the addition of TEA. At t = 0 min TEA was added to the bath solution, the response to depolarizing pulse potentials declined exponentially in time. Half time of the block by TEA was approximately three min.

related to the movement of a gating charge (z) causing a tiny gating current (Hille, 1984). A conformational change moves a gating charge of valence z from one side of the membrane to the other across the full membrane potential drop E. Let ω be the conformational energy increase upon opening of the channel in the absence of a membrane potential ($E = 0$). Along with the membrane potential the electrical energy of opening increases with $-zeE$, where e is the elementary charge. The total energy change thus is $\omega - zeE$. The Boltzmann equation gives the ratio of open (O) to closed (C) channels at equilibrium in terms of energy change:

$$O/C = \exp(-(\omega - zeE)/kT) \quad (1)$$

Here k is the Boltzmann's constant and T the absolute temperature on the Kelvin scale. Note that the ratio O/C is equal to the ratio α/β. All conformational changes must obey the Boltzmann equation of statistical mechanics. Consequently the transition rates α and β are bound by physical laws that can be expressed as the relative probability of finding a channel in an open (O) or closed (C) state at a given potential:

$$P_{open} = O/(C + O) \quad (2a)$$

and thus:

$$P_{open} = \alpha/(\alpha + \beta) \quad (2b)$$

combining Eqs. 1 and 2a the probability of finding channels, as presented in scheme 1, in an open state is:

$$P_{open} = 1/(1 + \exp[\{\omega - zeE\}/kT]) \quad (3a)$$

If ω is equal to zeE then $P_{open} = 0.5$. At this potential E is equal to ω/ze that is defined as $V_{1/2}$ thereby changing Eq. 3a into:

$$P_{open} = 1/(1 + \exp[\{V_{1/2} - E\} \cdot ze/kT]) \quad (3b)$$

This equation yields open probability values between zero and one, however the open probability may in reality vary over a smaller range (e.g., between 0.2 and 0.8) in which case one should use P'_{open} defined as:

$$P'_{open} = P_{max} \cdot [P_{min} + (1 - P_{min}) \cdot P_{open}] \quad (3c)$$

with $0 \leqslant P_{min}$ and $P_{max} \leqslant 1$.
Hodgkin and Huxley (1952) formulated the voltage dependence of α as:

$$\alpha = \alpha_o \cdot (V_\alpha - E)/(\exp[\{V_\alpha - E\}/S_\alpha] - 1) \quad (4)$$

Where α_o is the scaling factor, V_α determines the voltage dependence and S_α the steepness of the voltage dependence of α. According to Eq. 2b β can be calculated from α and P_{open} by:

$$\beta = \alpha/P_{open} - \alpha \quad (5)$$

Ion channels with simple kinetics (scheme 1) respond to changes in potential by a change in the ratio α/β resulting in a single exponential increase or decrease in current. The time dependence (τ) of whole cell activation and deactivation of these ion channels can directly be obtained by analysis of the corresponding curves. τ is voltage dependent because it is a fraction of α and β by:

$$\tau = 1/(\alpha + \beta) \quad (6a)$$

Eqs. 2b and 6a permit the expression of τ as a function of P_{open} and α:

$$\tau = P_{open}/\alpha; \tag{6b}$$

Eqs. 6a and 6b are only valid for channels represented by Scheme 1. Note that the open probability of the ion channel ($P_{open,ch}$) and the gate ($P_{open,g}$) are the same if only one gate is involved in the opening of an ion channel.

Steady State Open Probabilities for Linear HH Models

The deactivation curves in Figs. 1 and 2 follow single exponential curves suggesting that the activated ion channels have only one open state. The sigmoidal activation curves show that the rapidly activated channel, ORC-f, must have more than one closed state. Usually ion channels have one open state and many closed states (Gradmann & Bertl, 1989). For the analysis of such kinetics linear HH-models with p closed states are generally used (Hodgkin & Huxley, 1952).

$$C_1 \underset{\beta}{\overset{p\alpha}{\rightleftarrows}} C_2 \underset{2\beta}{\overset{(p-1)\alpha}{\rightleftarrows}} C_3 \ldots C_{p-1} \underset{(p-1)\beta}{\overset{2\alpha}{\rightleftarrows}} C_p \underset{p\beta}{\overset{\alpha}{\rightleftarrows}} O$$

Scheme 2a

As will be discussed further on Scheme 2a with four closed states (p = 4) describes best the rapidly activated ORC-f and with one closed state (p = 1, =Scheme 1) the slowly activated ORC-sp.

The open probability of an ion channel with p closed states ($P_{open,ch(p)}$) as depicted in scheme 2a can be calculated from the Boltzmann distribution (Eq. 3b) that determines the ratio of α over β. The open probability of an ion channel with p gates ($P_{open,ch(p)}$) is equal to $[P_{open,g}]^p$. Alternatively $P_{open,ch(p)}$ can also be calculated from the transition rate ratio's (*see below*). This approach allows for the calculation of $P_{open,ch(p)}$ if the linear HH-model is extended with one state that has different gating constants, here α' and β' (Scheme 2b).

$$C_1 \underset{\beta}{\overset{p\alpha}{\rightleftarrows}} C_2 \underset{2\beta}{\overset{(p-1)\alpha}{\rightleftarrows}} C_3 \ldots C_{p-1} \underset{(p-1)\beta}{\overset{2\alpha}{\rightleftarrows}} C_p \underset{p\beta}{\overset{\alpha}{\rightleftarrows}} O \underset{\beta'}{\overset{\alpha'}{\rightleftarrows}} Cx$$

Scheme 2b

As follows from Scheme 2a the sequence of the ratio's between the states $C_1{:}C_2{:}\cdots{:}C_p{:}O$ is given by:

$$1{:}C_1 \cdot [p\alpha/\beta]{:}C_2 \cdot [(p-1)\alpha/2\beta]{:}\cdots{:} C_{p-1} \cdot [2\alpha/(p-1)\beta]{:}C_p \cdot [\alpha/p\beta] \tag{7}$$

In steady state $P_{open,ch(p)}$ is equal to the ratio of $[\alpha/p\beta]$ over the sum of the ratios:

$$P_{open,ch(p)} = C_p \cdot [\alpha/p\beta]/(1 \times C_1 \cdot [p\alpha/\beta] + \cdots + O \cdot [\alpha/p\beta]) \tag{8}$$

A change in potential (from V_1 to V_2) causes a change of the steady state $P_{open,ch(p)}$ value by:

$$\delta P_{open,ch(p,V1,V2)} = P_{open,ch(p,V2)} - P_{open,ch(p,V1)} \tag{9}$$

Dynamic Currents: Activation and Deactivation

Changing V_m may cause an increase in current in time resulting in a final value of $P_{open,ch(p)}$ (Eq. 8). For linear HH-models an increase in current can accurately be described with the activation variable n^p_{act} (Hodgkin & Huxley, 1952):

$$n^p_{act} = [1 - \exp(-t/\tau_{act}]^p \tag{10}$$

This equation is only valid if the holding potential (V_h), preceding the activating pulse potentials, forced all channels in the C_1-state (Scheme 2). For channels with one open state τ_{act} is identical with τ (Eq. 6).

The time dependence of whole cell deactivation or tail currents (τ_{dea}) are determined by $p \cdot \beta$ if $\beta \gg \alpha$ (Scheme 2). Again p represents the number of closed states:

$$\tau_{dea} \approx 1/p \cdot \beta \tag{11}$$

A decrease in conductance caused by deactivation can be described with a single exponential curve:

$$n_{dea} = \exp(-t/\tau_{dea}) \tag{12}$$

When potassium currents are activated in whole cell the K^+ conductance ($G_{K(act)}$) depends on the total amount of K^+ channels present in the membrane (N), the conductance of the individual K^+ channels ($G_{K(sc)}$), the activation variable n^p_{act} and $P_{open,ch(p)}$:

$$G_{K(act)} = G_{K(sc)} \cdot N \cdot P_{open,ch(p)} \cdot n^p_{act} \tag{13}$$

If the maximum conductance $G_{K(max)}$ is the product of N and $G_{K(sc)}$ then:

$$G_{K(act)} = G_{K(max)} \cdot P_{open,ch(p)} \cdot n^p_{act} \tag{14}$$

Current passing through G_K is driven by δV_K, defined as the difference between the V_m and E_K and thus:

$$I_{K(act)} = \delta V_K \cdot G_{K(act)} \tag{15}$$

The initial open probability of the K^+ channels upon deactivation is equal to the open probability after the preceding activation pulse. The total activation time (at) thus determines the initial conductance at the start of deactivation. The final conductance after deactivation is

determined by $P_{\text{open,ch(p,Vdea)}}$ (Eq. 8). The deactivation potential causes a decrease in conductance by:

$$G_{\text{K(dea)}} = G_{\text{K(max)}} \cdot ([P_{\text{open,ch(p,Vact)}} \cdot n^{p}_{\text{act(at)}} - P_{\text{open,ch(p,Vdea)}}] \cdot N_{\text{dea}} + P_{\text{open,ch(p,Vdea)}}) \quad (16)$$

If the preceding activation time is long enough for the K^+ conductances to reach steady state (*see* Eq. 9) Eq. 16 becomes:

$$G_{\text{K(dea,ss)}} = G_{\text{K(max)}} \cdot (\delta P_{\text{open,ch(p,Vact,Vdeac)}} \cdot n_{\text{dea}} + P_{\text{open,ch(p,Vdea)}}) \quad (17)$$

Where ss refers to the preceding steady state condition during activation. The deactivation current follows:

$$I_{\text{K(dea)}} = \delta V_K \cdot G_{\text{K(dea)}} \quad (18)$$

Eqs. 15 and 18 predict the changes in current after a pulse potential and combine the kinetic model with the Boltzmann Distribution (Eq. 3*b*) and α (Eq. 4). This makes it possible to fit a set of activation and deactivation curves over a wide range of potentials (ensemble fit). In order to fit the experimental data using these equations the instantaneous changes in whole cell current, following the pulse potential are assumed to be conducted by leak conductances and were ignored for the analysis of channel kinetics.

Determination of the Kinetic Model of ORC-f and ORC-sp

Activation curves from single channel and whole cell data were used to find the *p* value for ORC-f and ORC-sp. From a V_h of −120 mV pulses of +160 mV were applied in the OOP configuration. This depolarization activated both ORC-f and ORC-sp conductances. From six recordings the datapoints originating from the baseline of the activation curve were collected (Fig. 5*A*). Using only datapoints from the baseline and not from single channel openings (*see* Fig. 2) ensures that the current is not carried by ORC-f but only by ORC-sp. The baseline current is conducted by the ORC-sp and corresponds with the activation variable m^p. Eq. 15 was fitted to the activation current. The best fit yielded a *p*-value of 0.927 ± 0.093. As *p* represents the number of closed states, *p* value can only be a whole number. A *p* value of 0.927 thus indicates one closed state for ORC-sp. $I_{\text{max(m)}}$ was 4.08 ± 0.07 pA and $\tau_{\text{act(m)}}$ 533 ± 32 msec.

Figure 5*B* shows three activation curves of a single whole cell. Their high signal/noise ratio and large amplitude, made them suitable for testing the *p* value of ORC-f in whole cell. The activation currents were fitted with the equation:

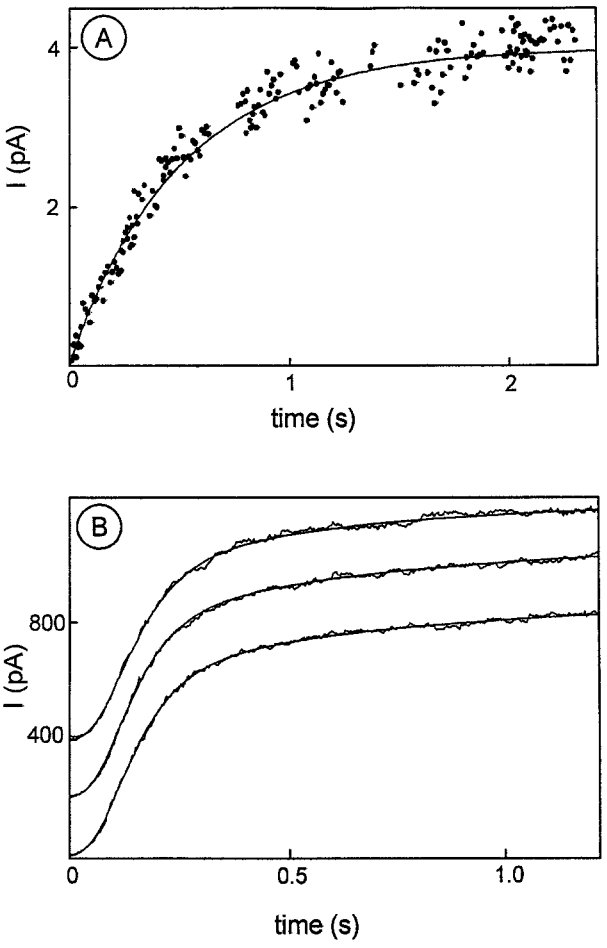

Fig. 5. (*A*) Baseline shift in outside-out patch configuration resulting from a depolarizing pulse of 160 mV, the holding potential was −120 mV. The data result from six similar pulse potentials applied to the same patch. All data corresponding to channel (ORC-f) openings were omitted. The curve was best fitted with a HH-model containing one closed state (m^1). (*B*) Three whole cell recordings from one cell of the depolarization activated K^+ current. The applied pulse was 135 mV more positive than the holding potential (−100 mV). The curves were best fitted with a double HH-model containing two conductances with one open and four closed states ($m^1 + n^4$).

$$I = I_{\text{max(m)}} \cdot [1 - \exp(-t/\tau_{\text{act(m)}})]^1 + I_{\text{max(n)}} \cdot [1 - \exp(-t/\tau_{\text{act(n)}})]p \quad (19)$$

with ORC-sp represented as m^1 and ORC-f as n^p. The free running *p* value was 4.01 ± 0.020, indicating four closed states. The values of $I_{\text{max(n)}}$ and $I_{\text{max(m)}}$ were 550 ± 17 pA and 300 ± 14 pA respectively indicating a significant contribution, here 35%, of the ORC-sp to the total outward current. The time constants $\tau_{\text{act(n)}}$ and $\tau_{\text{act(m)}}$ were 76.3 ± 2 msec and 578 ± 59 ms respectively. At this membrane potential the ORC-f time response is 7.5 times faster than that of the ORC-sp.

The deactivation curves (Figs. 1 and 2) are clearly first order, indicating that both conductances have only one open state. We conclude that Scheme 1 is the best

kinetic model for ORC-sp consisting one open and one closed state. The kinetic model for the ORC-f consists one open and four closed states (Scheme 3).

$$C_1 \underset{\beta}{\overset{4\alpha}{\rightleftarrows}} C_2 \underset{2\beta}{\overset{3\alpha}{\rightleftarrows}} C_3 \underset{3\beta}{\overset{2\alpha}{\rightleftarrows}} C_4 \underset{4\beta}{\overset{\alpha}{\rightleftarrows}} O \qquad \text{Scheme 3}$$

Effect of ORC-f Channel Flickering on Whole Cell Currents

Examples of flicker activity are depicted in Fig. 2 (OOP) and Fig. 6*A* (CAP) and have been reported before (Vogelzang & Prins, 1994). Flickering was observed with inward currents but not with outward currents. The flickering behavior conflicts with the five state model proposed in Scheme 3. When flickering was observed the open and closed times were of the same magnitude and very small, between 1 and 6 msec (Fig. 6*A*), much smaller than can be expected from τ_{dea} in whole cell (between 70 and 500 ms). Also if $4\beta \approx \alpha$ (Scheme 3) than, in steady state, $P_{open,ch(4)}$ would be greater then 0.3 (calculated for a five state HH-model), but $P_{open,ch}$ was less than 0.05 under whole cell steady state conditions. Clearly the introduction of an additional closed state is required as shown in Scheme 4:

$$C_1 \underset{\beta}{\overset{4\alpha}{\rightleftarrows}} C_2 \underset{2\beta}{\overset{3\alpha}{\rightleftarrows}} C_3 \underset{3\beta}{\overset{2\alpha}{\rightleftarrows}} C_4 \underset{4\beta}{\overset{\alpha}{\rightleftarrows}} O \underset{\beta'}{\overset{\alpha'}{\rightleftarrows}} C_f \qquad \text{Scheme 4}$$

Therefore, where α' and β' are transition rates between the open and the fifth closed state (C_f). The C_f- state may be positioned on either side of the open state. Neither whole cell nor single channel data could provide an indication of which position C_f is most likely, we have arbitrarily chosen for the right-side position.

The total time spent in open and closed state during flickering was used to calculate the Boltzmann distribution from six CAP experiments, $\Sigma time_{(open)}$ and $\Sigma time_{(closed)}$ during periods of flicker were estimated by fitting the frequency histograms of the corresponding flicker currents with gaussian functions (Fig. 6*B*). The ratio of $\Sigma time_{(open)}$ over $\Sigma time_{(open+closed)}$ was calculated at potentials ranging from 20 to 100 mV more negative then V_r (Fig. 6*C*). The values of the open probability of the flicker gate, $P_{open,g(f)}$, parameters were (Eq. 3): $z = 1.2 \pm 4$, $V_{1/2} = -22 \pm 4$ (mV) and $P_{min} = 0.44 \pm 0.05$, assuming a P_{max} value of one.

For a set of data from one experiment the voltage dependence of α' and β' was examined at potentials ranging from 20 to 85 mV more negative than V_r. The corresponding mean open and closed times during flickering are depicted in Fig. 7. The reciprocal of mean open and closed time are equal to β' and α' respectively. Clearly both α' and β' were voltage dependent. The α'

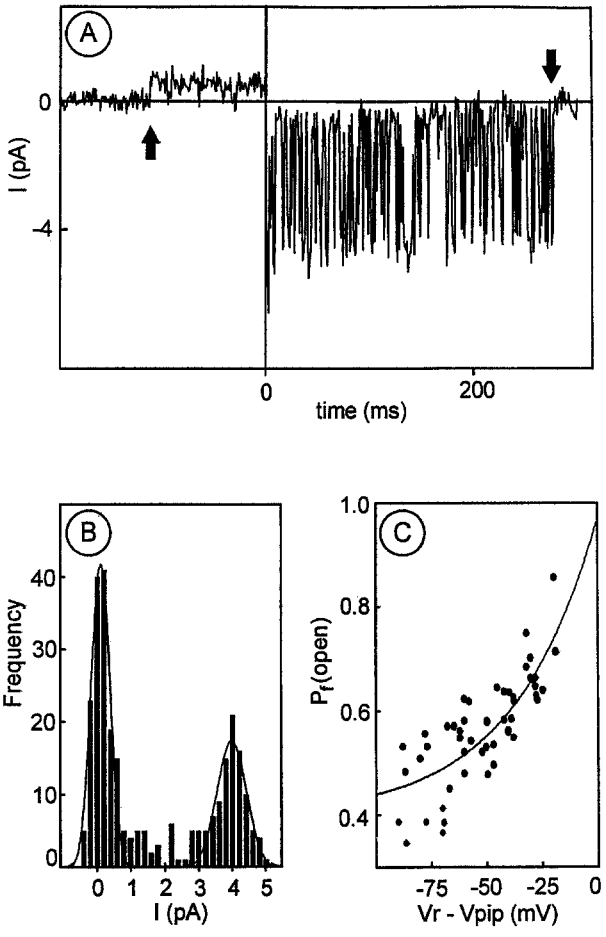

Fig. 6. (*A*) Single channel current in cell attached patch configuration displaying the opening of an ORC-f at 0.1 sec (arrow upward) before a hyperpolarizing pulse potential (90 mV) was applied. This hyperpolarizing potential caused a flickering inward current. After 0.3 sec, the flickering stopped completely (arrow downward). According to the six-state model (Scheme 4) this flickering is caused by fast transitions between the open and the C_f state. (*B*) Frequency histograms of flicker currents. The data were collected within periods of channel flickering. The $\Sigma time_{(open)}$ over $\Sigma time_{(closed)}$ was estimated by fitting the frequency histograms with two gaussian functions. (*C*) The ratio of $\Sigma time_{(open)}$ over $\Sigma time_{(open+closed)}$ was plotted versus the difference between V_r and the pipette potential (V_{pip}) for six different protoplasts. The data were fitted with a Boltzmann distribution function (Eq. 3).

curve was described with an arbitrary equation similar to Eq. 4 but with two modifications. At negative going potentials α' reached a steady value that was well above zero and β' reached a steady value of about 0.5. Therefore a minimum value for α' (α'_{min}) had to be added to Eq. 4. The second modification was the exclusion of $V_{\alpha'}$. The parameters of the α' and Boltzmann equation were fitted separately (Boltzmann's points were calculated from β' and α', *see* Eq. 5) resulting in $\alpha'_o = 0.07 \pm 0.04$ ($mV^{-1}msec^{-1}$), $S_{\alpha'} = 13 \pm 5$ (mV), $\alpha'_{min} = 0.36 \pm 0.06$ ($mV^{-1}msec^{-1}$) and for $P_{open,g(f)}$:$z = 1.49 \pm 0.15$, $V_{1/2} = -28 \pm 1$ (mV) and $P_{min} = 0.40 \pm 0.02$.

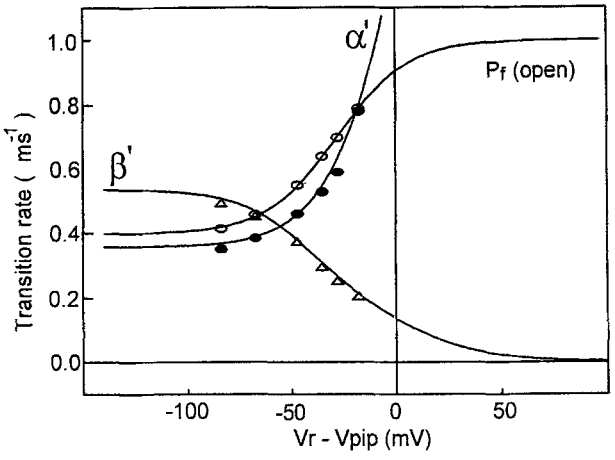

Fig. 7. Mean open and closed times during channel flickering were determined at potentials ranging from −85 to −15 mV for one cell in the cell attached patch configuration. The reciprocal values, respectively α' and β' were calculated and plotted versus the difference between V_r and the pipette potential (V_{pip}) together with the corresponding Boltzmann distribution (Eq. 2).

Even at activation potentials with a small τ_{act} value (76 ± 2 ms, Fig. 5*B*) α' was about 60 times greater than α. Apparently at potentials more positive than E_K, the C_f-state had no effect on the shape and time response of the activation curves and the model proposed in Scheme 3 was still valid for activation curves. However, if, $\beta \gg \alpha$, then τ_{dea} will increase proportional to the $(\alpha' + \beta')/\alpha'$ ratio (Colquhoun & Hawkes, 1977), for Scheme 4:

$$\tau_{dea} = [(\alpha' + \beta')/\alpha'] \cdot [1/p \cdot \beta] \tag{20}$$

Extension of the linear model from Scheme 2 with an additional closed state (C_f) requires a reformulation of Eq. 8:

$$P_{open,ch(4+1)} = C \cdot [\beta'/\alpha'](1 + C_1 \cdot [p\alpha/\beta] + \cdots + C_4 \cdot [\alpha/4\beta] + O \cdot [\beta'/\alpha']) \tag{21}$$

Figures 6C and 7 show that P_{min} can vary between 0.3 to 0.5 resulting in an increase of τ_{dea} by 3.3 and 5 respectively.

Inclusion of Single Channel Current-Voltage Relationship

Ensemble fits must be corrected for the current-voltage relationship of the corresponding ion channels, unless this relation is linear within the pulse potential range and the applied ion activity on either side of the membrane. The actual K^+ current flowing through the ion channels in whole cell measurements depends on the conductance of individual ion channels and δV_K. The conductance of a single channel ($G_{K(sc)}$) usually follows a curve that saturates with increasing ion activity. The conductance of some K^+ channels in plant cells is strongly voltage dependent. This complicates the behavior of $G_{K(sc)}$. As a result the corresponding *I-V* curves are nonlinear. Such *I-V* curves can be accurately described with four-state translocator models for a variety of ionic gradients (Bertl, 1989; Gradmann, Klieber & Hansen, 1987; Hansen et al., 1981). These models describe the current as a function of voltage and ion activity. For the ORC-f the parameters of a four-state model were determined earlier (Vogelzang & Prins, 1994). K^+ currents in whole cell are predicted by Eq. 15 describing changes during activation. It includes $G_{K(sc)}$ and δV_K that are substituted, for ORC-sp, by the current predicted by the translocator model ($I_{K(sc,tr)}$):

$$I_{K(act)} = I_{K(sc,tr)} \cdot N_{(ORC\text{-}sp)} \cdot P_{open,ch(1,Vact)} \cdot n_{act}^1 \tag{22}$$

and for ORC-f:

$$I_{K(act)} = I_{K(sc,tr)} \cdot N_{(ORC\text{-}f)} \cdot P_{open,ch(4+1,Vact)} \cdot n_{act}^4 \tag{23}$$

A similar reasoning is valid for deactivation currents (Eq. 18) for ORC-sp:

$$I_{K(dea} = I_{K(sc,tr)} \cdot N_{(ORC\text{-}sp)} \cdot (\delta P_{open,ch(1,Vact,Vdeac)} \cdot n_{dea} + P_{open,ch(1,Vdea)}) \tag{24}$$

and for ORC-f:

$$I_{K(dea,n)} = I_{K(sc)} \cdot N_{(ORC\text{-}f)} \cdot (\delta P_{open,ch(4+1,Vact,Vdeac)} \cdot n_{dea} + P_{open,ch(4+1,Vdea)}) \tag{25}$$

Ensemble Fit of Simultaneously Depolarization Activated K^+ Currents

ORC-f currents were predicted with Eq. 23 and Eq. 25 that contain five parameters originating from α and the Boltzmann function for open probability. Two extra parameters were required for the ensemble analysis of ORC-f: $N_{(ORC\text{-}f)}$ for the number of ORC-f channels and P_{min} for the flicker open probability. Eq. 22 and Eq. 24 were used for the simulation of the ORC-sp. Initially it was assumed that the shape of the single channel *I-V* curve was the same for both the ORC-sp and ORC-f, because both channels share ion selectivity, voltage sensitive activation and voltage dependent gating. However, stable fits were only obtained if the inward current through ORC-sp was increased by a factor Φ. This together with $N_{(ORC\text{-}sp)}$ for the number of ORC-sp channels makes the total number of parameters for ORC-sp seven. Note that $\Phi > 1$ makes the single channel I-V curve of the ORC-sp more asymmetric than that of ORC-f, i.e., the ratio between inward and outward conductance is increased, favoring the inward current. $N_{(ORC\text{-}f)}$ and

Table 1. Results of ensemble fit

Parameters	ORC-f			ORC-sp		
	Mean	σ_{fit} = Dσ Min	Max	Mean	σ_{fit} = Dσ Min	Max
α_o (mV^{-1} sec^{-1})	2.1E-1	1.2E-1	3.5E-1	3.3E-2	2.1E-2	5.4E-2
$V_\alpha - E_K$ (mV)	−1.0E1	−3.9E1	−4.0E0	−1.7E1	−2.2E1	−1.4E1
S_α (mV)	8.5E0	6.6E0	1.4E1	5.5E0	5.0E0	6.1E0
z	1.9E0	1.4E0	2.8E0	3.7E0	3.4E0	4.2E0
$V_{1/2} - E_K$ (mV)	−1.9E1	−3.1E1	−7.3E0	−1.1E1	−1.5E1	−7.3E0
N	4.3E2	3.6E2	4.7E2	1.4E2	1.0E2	1.6E2
Φ				3.1E0	2.3E0	3.6E0
P_{min}	3.4E-1	0.0E0	7.9E-1			

The standard error, σ_{fit}, of the best fit from one cell was 0.43 pA. Dσ is the double value of the minimal σ_{fit}. The values of the parameters were decreased or increased until σ_{fit} equalled Dσ. The sensitivity of the fit per parameter is thus indicated by the minimal (min) and maximal (max) values. 329 datapoints were used for the ensemble analysis of one cell.

$N_{(ORC\text{-}sp)}$ have a slightly different meaning. Where $N_{(ORC\text{-}f)}$ is the absolute number of ORC-f channels in one cell (430 for the data shown in Table 1), $N_{(ORC\text{-}sp)}$ is defined relative to $N_{(ORC\text{-}f)}$. The value of 140 for $N_{(ORC\text{-}sp)}$ indicates in fact that 140 ORC-f channels would be required to match the conductance through the ORC-sp channels. It was assumed that all α and $P_{open,g}$ functions depend on E_K, therefore E_K was added to E in Eq. 3a and Eq. 4.

Whole cell recordings from three cells with equal E_K values (−55 mV) were fitted simultaneously to estimate the value of the fourteen parameters. Each cell was given its own $N_{(ORC\text{-}sp)}$, $N_{(ORC\text{-}f)}$, Φ and P_{min} value. The values obtained for the different parameters are given in Table 1. The $N_{(ORC\text{-}sp)}$, $N_{(ORC\text{-}f)}$, Φ and P_{min} values originate from the whole cell recording shown in Fig. 8. For the sake of clarity, in this figure the datapoints of only one recording are shown. The activation and deactivation curves generated by the ensemble model (of these cells) are shown by the drawn lines in the same picture. The standard error of the best fit, σ_{fit}, was 0.43 pA. The sensitivity of the fit for each single parameter was examined by testing to what value it had to be increased, or decreased, to double the originally observed σ_{fit}. The therefore required parameter values are given in the column (Table 1) indicated by Dσ (''double sigma'').

As expected, the transition rate α or the ORC-f is greater than that of the ORC-sp, both the scaling factor (α_o) and steepness (S_α) of the ORC-sp are smaller. The gating charge of the ORC-sp (3.7) was almost twice that of ORC-f (1.9). For both, ORC-f and ORC-sp, V_α and $V_{1/2}$ were not significantly different. Also V_α of ORC-f and ORC-sp differed not significantly, this was also true for $V_{1/2}$. P_{min} from the ensemble fit was 0.34. Analysis of single channel data of channel flickering (*see above*) also yielded P_{min} values higher than zero. The P_{min} value obtained from the analysis of the ratio of $\Sigma time_{(open)}$ over $\Sigma time_{(open+closed)}$ was 0.40, the P_{min} value from the α and Boltzmann analysis was 0.44. $N_{(ORC\text{-}f)}$ was 3.1 times greater then $N_{(ORC\text{-}sp)}$. It is remarkable that this difference is almost fully compensated for inward currents by Φ that increases the inward current of ORC-sp by 3.1.

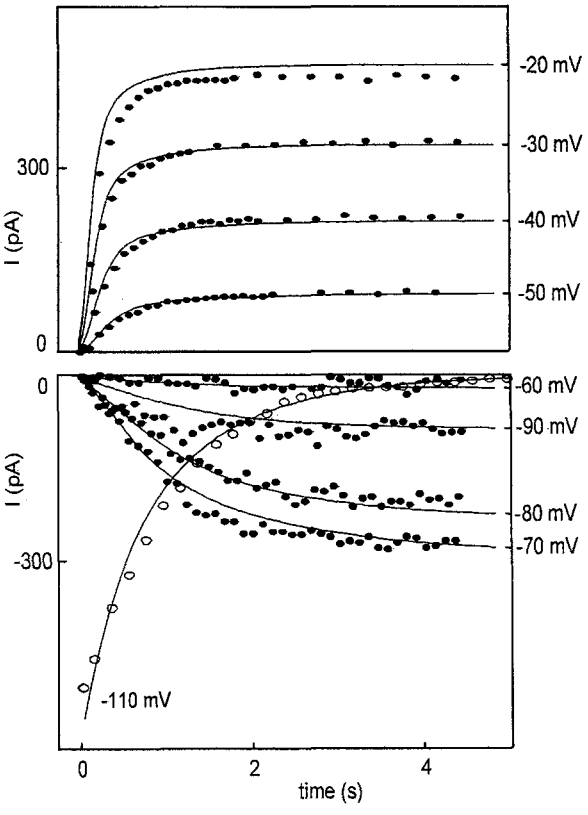

Fig. 8. Datapoints used for the ensemble fit are plotted in the upper and lower graph. Datapoints corresponding with activation curves are plotted as closed circles, those of deactivation curves as open circles. The inward currents of the activation curves are multiplied by five for clarity, the deactivation data are not. The lines represent the result of the ensemble fit of three different cells.

Discussion

The starting hypothesis for the present analysis was the presence of two separate K^+ conducting ORC's with an E_K dependent activation. The outcome of this analysis shows that the data can indeed be described best by a model containing two ORCs: ORC-f with a rapid sigmoidal activation and four plus one closed states, and ORC-sp with a slow exponential activation with one closed state and both with one open state. The analysis thus supports the starting hypothesis.

Sigmoidal-activation and exponential-deactivation outward potassium currents have been observed in most plant protoplasts studied so far (Schroeder, Hedrich & Fernandez, 1984; Schroeder, Raschke & Neher, 1987; Moran, Fox & Satter, 1990; Colombo & Cerana, 1991; Fairley-Grenot, Laver & Walker, 1991; Ketchum & Poole, 1991; Schachtman et al., 1991; Van Duijn et al., 1992 etc.). A quantitative analysis of outward rectifying currents in plants was first described by Schroeder (1989) for guard cells of *V. faba.* A similar analysis was reported by Van Duijn (1993) for outward rectifying currents of tobacco cultured cells. Van Duijn compared both currents and concluded that both can be described with a similar n^2 HH-model but that the parameters showed important quantitative differences. Clearly the kinetics of the ORC-f (n^4) and ORC-sp (m^1) in the present study differ from the n^2 channels of Schroeder (1989) and Van Duijn (1993).

The ensemble analysis reported here is based on a model that uses two voltage-dependent functions that describe ion channel kinetics in whole cell. These functions are the Boltzmann equation and α. The analysis reported here is different from the original work of Hodgkin and Huxley (1952) in that the process of analysis is reversed. Hodgkin and Huxley analyzed activation and deactivation currents showing that the corresponding time responses were voltage dependent. Firstly, they calculated the parameters of the Boltzmann equation and the functions describing the voltage dependence of activation and deactivation times separately. From these three functions, the voltage-dependent rate of ion channel state transition from respectively closed to open state (α) and open to closed state (β) were calculated. In the present work, the Boltzmann equation and the α function were used as a starting-point for the characterization of the outward rectifying currents. The combination of these functions creates a model that generates both activation and deactivation curves. Single channel recordings of the ORC-f revealed fast channel kinetics (flickering) that affect the time constants of whole cell tail currents and thus the kinetic of deactivation (Eq. 20). Therefore the gating properties responsible for flickering were added to the ORC-f model. To describe the whole cell data adequately the functions describing single channel *I-V* curve characteristics were added to the model. Therefore the ORC-f translocator model was used (Vogelzang & Prins, 1994). An ensemble analysis is complex but attractive because it reduces the number of parameters required to describe channel kinetics. In addition, it is a test for the HH-models presented for ion channels in general. Finally, it allows fitting of two parallel outward rectifying currents which are difficult to separate.

The asymmetrical shape of the single channel *I-V* curve of the ORC-f, favoring inward currents, had to be adapted for the ORC-sp. To further increase the inward going current of the ORC-sp Φ was introduced. The preference of the ORC-f for inward currents, e.g., 40 pS inward versus 25 pS outward (Vogelzang & Prins, 1994), can be expressed as the inward/outward ratio. For the ORC-f this ratio is 1.6. For the ORC-sp this value has to be multiplied by Φ (Table 1) resulting in an inward/outward ratio of 5.0.

The low sensitivity of the model for some of the parameters (Table 1) may indicate that either the model is incomplete or that the data used for the ensemble fit should be collected over a greater voltage domain, especially at more negative potentials. The ensemble model will be used for simulations of dynamic electrical behavior of inward and outward rectifying currents in whole cell current and voltage clamp configurations. Such ensemble models are required for the analysis the dynamics of V_m, I_m or g_m which can change significantly if proton pump activity is stimulated by addition of hormone like compounds (e.g., fusicoccine) or by changes in light conditions (Blom et al., 1994). Preliminary experiments indicate that the ensemble model produces realistic behaviour of V_m in current clamp and I_m in voltage clamp but that slightly higher values are required for S_α (ORC-f and ORC-sp).

In Table 2, the data of *P. media* root cells are given together with those from Hodgkin and Huxley (1952), Schroeder (1989) and Van Duijn (1993). The transition rate constants for gating of plant ion channels are much smaller than those found for K^+ channels in nerve cells. The α_o parameter of both *P. media* ORCs are comparable with those of tobacco and much smaller than α_o of ion channels in nerve cells. V_α of the ORC-sp and ORC-f of *Plantago* are more negative than the V_α values of the ORC of tobacco (>90 mV) and of nerve cells (>70 mV). In contrast the S_α values are very close varying between 6 and 10 mV. The gating charge of the ORC-sp and ORC-f are respectively four and two times that of tobacco and *Vicia* ORCs. The $V_{1/2}$ values of the *P. media* ORCs are more negative than those of *Vicia* (>50 mV), tobacco (>90) and nerve cells (>70). Both the ORC-f and the ORC in nerve cells have four closed states. The ORC-sp is the only channel with one closed state.

The physiological function of the K-state created by E_K gated K^+ channels in root cells might be to maintain a constant K^+ conductance over a wide range of E_K val-

Table 2. Comparison of parameters of the α function and the Boltzmann distribution

	α_o mV^{-1} sec^{-1}	V_α mV	S_α mV	z	$V_{1/2}$ mV	gates
ORC-sp	0.03	−72	6	3.7	−66	1
ORC-f	0.21	−65	9	1.9	−74	4[a]
Vicia faba[b]	—	—	—	1.2	−7	2
Tobacco[c]	0.112	29	9	0.9	28	2
Nerve[d]	10	10	10	1.5	14	4

Parameters of α-function and the Boltzmann distribution of outward rectifying currents of different origin are presented with the number of identified gates. For comparison E_k (here −55 mV) has not been subtracted from the $V_{1/2}$ and V_α val;ues of ORC-sp and ORC-f.

[a] The gate responsible for flickering is not included.

[b] The α function used by Schroeder (1989) is not suitable for comparison.

[c] Van Duijn (1993).

[d] Hodgkin and Huxley values for the K^+ conductance n in nerve cells. $V_{1/2}$ and z have been calculated from the given parameters for the α and β functions (Hodgkin & Huxley, 1952).

ues. Variations of the apoplastic K^+ concentration may cause E_K, and therefore V_m, to change without large effects on the K^+ conductance. For cells in the K-state any efflux of protons by the H^+-ATPase pump causes a slight hyperpolarisation of V_m thereby driving K^+ ions from apoplast into the cytosol.

We thank Dr. P.J.C. Kuiper for his enthusiastic support of this research and critical reading of the manuscript. This research was supported by the former Foundation for Biophysics (now SLW), part of the Dutch Organization for Scientific Research (NWO).

References

Beilby, M.J. 1986. Factors controlling the K^+ conductance in *Chara*. *J. Membrane Biol.* **93:**187–193

Bertl, A. 1989. Current-voltage relationships of a sodium-sensitive potassium channel in the tonoplast of *Chara corallina*. *J. Membrane Biol.* **109:**9–19

Bisson, M.A., Walker, N.A. 1982. Transitions between modes of behaviour states of the charophyte plasmalemma. *In:* Plasmalemma and tonoplast: Their functions in the plant cell. D. Marmé, E. Marrè and R. Hertel, editors. pp. 35–40. Elsevier Biomedical B.V.

Blom-Zandstra, M., Koot, J.T.M., Hattum van, J. Vogelzang, S.A. 1994. Isolation of protoplasts for patch-clamp experiments: An improved method requiring minimal amounts of adult leaf or root tissue from monocotyledonous or dicotyledonous plants. *Protoplasma (in press)*

Bush, D.S., Hedrich, R., Schroeder, J.I., Jones, R.L. 1988. Channel-mediated potassium flux in barley aleurone protoplasts. *Planta* **176:**368–377

Caceci, M.S., Cacheris, W.P. 1984. Fitting curves to data: The simplex algorithm is the answer. *Byte* **5:**340–362

Colombo, R., Cerana, R. 1991. Inward rectifying K^+ channels in the plasma membrane of *Arabidopsis thaliana*. *Plant Physiol.* **97:** 1130–1135

Colquhoun, D., Hawkes, A.G., 1977. Relaxation and fluctuations of membrane currents that flow through drug-operated channels. *Proc. R. Soc. Lond.* **199:**231–262

Cruz-Mireles, R.M., Ortega-Blake, I. 1991. Effect of Na_3VO_4 on the P-state of Nitella translucens. *Plant Physiol.* **96:**91–97

Fairley-Grenot, K.A., Laver, D., Walker, N.A. 1991. Whole-cell and single-channel currents across the plasmalemma of corn shoot suspension cells. *J. Membrane Biol.* **121:**11–22

Gradmann, D., Bertl, A. 1989. Physiological control of membrane currents in plants. *Plant Physiol. Biochem.* **27:**587–593

Gradmann, D., Klieber, H.G., Hansen, U.P. 1987. Reaction kinetic parameters for ion transport from steady-state current-voltage curves. *Biophys. J.* **51:**569–585

Hagiwara, S., Miyazaki, S., Rosenthal, N.P. 1976. Potassium current and the effect of cesium on this current during anomalous rectification of the egg cell membrane of a starfish. *J. Gen. Physiol.* **67:**621–638

Hamill, O., Marty, A., Neher, E., Sakmann, B., Sigworth, F.J. 1981. Improved patch-clamp techniques for high-resolution current recording from cells and cell free membrane patches. *Pfluegers Arch.* **391:**85–100

Hansen, U.P., Gradmann, D., Sanders, D., Slayman, C.L. 1981. Interpretation of current voltage relationships for "active" ion transport systems: I. Steady state reaction-kinetic analysis of Class-I mechanisms. *J. Membrane Biol.* **63:**165–190

Hille, B. 1984. Classical biophysics of the squid giant axon. *In:* Ionic channels of excitable membranes. pp. 23–57. Sinauer Associates, Sunderland, Massachusetts

Hodgkin, A.L., Huxley, A.F. 1952. A quantitative description of membrane current and its application to conduction and excitation in nerve. *J. Physiol.* **117:**500–544

Ince, C., Van Dissel, J.T., Diesselhoff, M.M.C. 1985. A teflon culture dish for high magnification microscopy and measurements in single cells. *Pfluegers Arch.* **403:**240–244

Ketchum, K.A., Poole, R.J. 1991. Cytosolic calcium regulates a potassium current in corn *Zea mays*. protoplasts. *J. Membrane Biol.* **119:**277–288

Maathuis, F.J.M., Prins, H.B.A. 1990. Electrophysiological membrane characteristics of the salt tolerant *Plantago maritima* and the salt sensitive *Plantago media*. *Plant and Soil* **123:**233–238

Moran, N., Fox, D., Satter, R.L. 1990. Interaction of the depolarizing activated K^+ channel of *Amanea saman* with inorganic ions: a patch-clamp study. *Plant Physiol.* **94:**598–605

Schachtman, D.P., Tyermann, S.D., Terry, B.R. 1991. The K^+/Na^+ selectivity of a cation channel in the plasma membrane of root cells does not differ in salt-tolerant and salt-sensitive wheat species. *Plant Physiol.* **97:**598–605

Schroeder, J.I. 1989. Quantitative analysis of outward rectifying K^+ channel currents in guard cell protoplasts from *Vicia faba*. *J. Membrane Biol.* **107:**229–235

Schroeder, J.I., Fang, H.H. 1991. Inward-rectifying potassium channels in guard cells provide a mechanism for low-affinity potassium uptake. *Proc. Natl. Acad. Sci. USA* **88:**11583–11587

Schroeder, J.I., Hedrich, R., Fernandez, J.M. 1984. Potassium-selective single channels in guard cell protoplasts of *Vicia faba*. *Nature* **312:**361–362

Schroeder, J.I., Raschke, K., Neher, E. 1987. Voltage dependence of K^+ channels in guard-cell protoplasts. *Proc. Natl. Acad. Sci. USA* **84:**4108–4112

Skerret, M., Tyerman, S.D. 1994. A channel that allows inwardly directed fluxes of anions in protoplasts derived from wheat roots. *Planta* **192:**295–305

Terry, B.R., Tyerman, S.D., Findlay, G.P. 1991. Ion channels in the plasma membrane of Amaranthus protoplasts. One cation and anion channel dominate the conductance. *J. Membrane Biol.* **121:**223–236

Van Duijn, B. 1993. Hodgkin-Huxley analysis of whole-cell outward rectifying K^+ currents in protoplasts from tobacco cell suspension cultures. *J. Membrane Biol.* **132:**77–85

Van Duijn, B., Ypey, D.L., Van der Molen, L.G., Libbenga, K.R. 1992. Whole cell patch clamp experiments on tobacco protoplasts. *In:* Progress in Plant Growth Regulation. C.M. Karssen, L.C. van Loon and D. Vreugdenhil, editors. pp. 668–674. Kluwer Academic, Dordrecht, The Netherlands

Vogelzang, S.A., Prins, H.B.A. 1992. Plasmalemma patch clamp experiments in plant root cells: procedure for fast isolation of protoplasts with minimal exposure to cell wall degrading enzymes. *Protoplasma* **171:**104–109

Vogelzang, S.A., Prins, H.B.A. 1994. Patch clamp analysis of the dominant plasma membrane K^+ channel in root cell protoplasts of *Plantago media* L. Its significance for the P- and K- state. *J. Membrane Biol.* **141:**113–122